Evanescent Waveguide and Photochemical Characterization of Azobenzene-Functionalized Dendrimer Ultrathin Films

Derek Patton, Mi-Kyoung Park, Shuangxi Wang, and Rigoberto C. Advincula*

Department of Chemistry, University of Alabama at Birmingham, Birmingham, Alabama 35294-1240

Received October 8, 2001. In Final Form: December 12, 2001

In this work we describe the evanescent waveguide characterization and photoalignment of azobenzene-functionalized dendrimer ultrathin films. Azobenzene dyes were grafted to the perimeter of polyamidoamine dendrimers. The photoisomerization and photoalignment properties were first investigated in relation to solution and film. The dendrimers were then blended with polystyrene, which served as a matrix for this investigation. Planar waveguides were prepared by spin coating on Au−BK7 glass substrates. The waveguides were investigated by ATR methods characterizing the s and p components of the waveguides. The refractive indices of the films were sensitively determined. The anisotropy of the dielectric constants were found to be highly dependent on the dendrimer/polystyrene ratio and aggregation properties.

Introduction

Macromolecular systems containing photoresponsive units such as azobenzenes have been the subject of intense investigation in recent years. Many of the systems reported in the literature focus either on the incorporation of azobenzene molecules into a linear polymer chain as substituents or simply on doping the polymer with single azo-dyes.[1,2] In contrast to linear systems, dendrimers, a new class of macromolecules characterized by their treelike generational structure, have attracted increased attention with regard to design, synthesis, and functional chemistry.[3] This said, dendritic macromolecules containing photosensitive groups within their structure or at their perimeter have recently been reported.[4−6] The incorporation of a photochromic moiety in dendrimers is very attractive because of the possibility of creating new light-sensitive materials, storage, and optical devices. However, there have been few studies detailing the photochromic behavior of these materials as ultrathin films.[7,8]

A main interest of these azobenzene-containing polymer systems is their photoisomerization and birefringence properties. Birefringence is observed in these systems upon irradiation with linear polarized UV light (photoinduced alignment), which originates from light-induced isomerization cycles between the trans and cis configuration of the azo moiety. This results in a reorientation of the transition dipole of the chromophore into the direction perpendicular to the polarization direction of the incident light.[9] Several factors influence the photoisomerization process of azobenzene including the available free volume[10,11] and the aggregation state[12] of the chromophores, both being closely related. The effects of aggregation on the photoisomerization of azobenzenes have been studied using a variety of film preparation techniques including Langmuir−Blodgett (LB),[13,14] layer-by-layer,[15] and spin coating.[16] However, to our knowledge, there have been no reported studies with regards to the effect of aggregation on azobenzene-functionalized dendrimers and their photoalignment behavior by evanescent waveguide techniques.

In this context, we have investigated in the present study the effects of aggregation, phase separation, and molecular structure on the photoisomerization and photoalignment of an azobenzene-functionalized poly(amidoamine) (PAMAM−azo) dendrimer system. A three-generation (G3) PAMAM dendrimer was functionalized on the periphery with 32 azobenzene chromophores as shown in Figure 1. The synthesis is described below. To study the interactions of the PAMAM−azo in a polymer matrix, polystyrene was selected for several reasons. First, a polymer must be chosen so that both the solubility of the polymer and the solubility of the PAMAM−azo are suitable to a common solvent (miscible). Second, the polymer must yield a homogeneous film by the spin-coating technique and be optically transparent for those wavelengths that PAMAM−azo is expected to absorb. Finally, the polymer must interact with the PAMAM−azo in such a way as to provide the desired phase separation and aggregation characteristics which will substantially differentiate the blend system from the pure PAMAM−azo system. To this we have found the PAMAM−azo/polystyrene to be suitable for our purpose. Several analysis techniques were used to characterize the three systems (100% PAMAM−azo, 50% PAMAM−azo/PS, 5% PAMAM−azo/PS) in this study. Polarized UV−vis spectroscopy was utilized to follow the

(1) Wu, Y.; Kanazawa, A.; Shiono, T.; Ikeda, T.; Zhang, Q. *Polymer* **1999**, *40*, 4787.
(2) Wang, G.; Gan, F. *Mater. Lett.* **2000**, *43*, 6.
(3) Moorefield, C. N.; Vogtle, F. *Dendritic Molecules: Concepts, Syntheses and Perspectives*; VCH: Weinheim, Germany, 1996.
(4) Junge, D.; McGrath, D. *J. Am. Chem. Soc.* **1999**, *121*, 4912.
(5) Archut, A.; Azzellini, G.; Balzani, V.; De Cola, L.; Vogtle, F. *J. Am. Chem. Soc.* **1998**, *120*, 12187.
(6) Jiang, D.; Alda, T. *Nature* **1997**, *388*, 454.
(7) Sidorenko, A.; Houphouet-Boigny, C.; Villavicencio, O.; Hashemzadeh, M.; McGrath, D.; Tsukruk, V. *Langmuir* **2000**, *16*, 10569.
(8) Weener, J.-W.; Meijer, E. W. *Adv. Mater.* **2000**, *12*, 741.
(9) Buffeteau, T.; Labarthet, F.; Pezolet, M.; Sourisseau, C. *Macromolecules* **1988**, *21*, 7312.
(10) Haitjema, H.; Morgen, L.; Tan, Y.; Challa, G. *Macromolecules* **1994**, *27*, 6201.
(11) Paik, C. S.; Morawetz, H. *Macromolecules* **1972**, *5*, 171.
(12) Advincula, R.; Fells, E.; Park, M. *Chem. Mater.* **2001** *13*, 2870.
(13) Song, X.; Perlstein, J.; Whitten, D. *J. Am. Chem. Soc.* **1997**, *119*, 9144.
(14) Wang, R.; Yang, J.; Wang, H.; Tang, D.; Jiang, L.; Li, T. *Thin Solid Films* **1995**, *256*, 205.
(15) Saremi, F.; Tieke, B. *Adv. Mater.* **1998**, *10*, 388.
(16) Labarthet, F.; Freiberg, S.; Pellerin, C.; Pezolet, M.; Natansohn, A.; Rochon, P. *Macromolecules* **2000**, *33*, 6815.

10.1021/la015622s CCC: $22.00
Published on Web 01/23/2002

photoisomerization process while linear polarized photoisomerization was used to study photoinduced alignment of the azobenzene chromophores. To probe the optically induced anisotropy in the films in detail, attenuated total reflection (ATR) waveguide spectroscopy[17,18] was used to obtain information about in- and out-of-plane refractive indices as a function of irradiation time. This technique involved the preparation of ultrathin films on highly reflecting surfaces such as Au with sufficient refractive index contrast to the dielectric film. In our case, the technique was limited to polystyrene films with a minimum thickness (≈700 nm) and planar homogeneity (±1 nm).

Experimental Section

Synthesis. *4-Hexyl-4′-hydroxyazobenzene (**1**).* 4-Hexylaniline (6 g, 33.9 mmol) was dissolved in 10 mL of concentrated HCl (120 mmol) and 50 mL of water and cooled to 0 °C in an ice bath. To this mixture, 2.4 g (33.9 mmol) of sodium nitrite was dissolved in 8 mL of water and was slowly added under constant stirring to keep the solution temperature below 5 °C. Upon addition of the sodium nitrite, all solid material was dissolved and the mixture was stirred at 0 °C for an additional 10 min. In a separate batch, 3.18 g (33.9 mmol) of phenol was dissolved in 60 mL (2 M) of aqueous sodium hydroxide and was also cooled to 0 °C. The diazonium solution was slowly added to the phenolate solution, resulting in a deep red colored solution. The solution was stirred at 8 °C for 1 h, during which a red precipitate formed and was stirred further for 4 h at room temperature. The red solid was filtered, washed thoroughly with water, and then dried. The crude product was purified by recrystallization from hexane. Yield: 7.2 g (75%). ^{1}H NMR ($CDCl_3$): 7.81 (2H, d, J = 8.9 Hz, Ar−H), 7.24 (2H, d, J = 8.3 Hz, Ar−H), 7.23 (2H, d, J = 8.3, Hz, Ar−H), 6.93 (2H, J = 9.0 Hz, Ar−H), 2.60 (2H, t, $-CH_2Ar$), 1.57−1.20 (6H, m, C_4H_6), 0.81 (3H, m, CH_3).

*Ethyl [4-(4′-Hexylphenylazo)phenyloxy]acetate (**2**).* Ethyl bromoacetate (1.67 g, 10 mmol) and 4-hexyl-4′-hydroxyazobenzene (2.82 g, 10 mmol) were mixed with powdered K_2CO_3 (2.1 g, 15 mmol) and a catalytic amount of KI, and the mixture was suspended in 150 mL of acetone. The mixture was refluxed with stirring for 12 h. After the solvent was removed, the residue was taken in dichloromethane and twice washed with water. After the organic fraction was dried over magnesium sulfate and dichloromethane removed, the obtained product was purified by recrystallization from hexane to 2.8 g (yield, 76%) of ethyl [4-(4′-hexylphenylazo)phenyloxy]acetate as an orange crystal. ^{1}H NMR ($CDCl_3$): 7.82 (2H, d, J = 8.9 Hz, Ar−H), 7.24 (2H, d, J = 8.3 Hz, Ar−H), 7.23 (2H, d, J = 8.3, Hz, Ar−H), 6.93 (2H, J = 9.0 Hz, Ar−H), 4.62 (2H, s, $-OCH_2-$), 4. 39 (2H, m, $-OCH_2-$), 2.60 (2H, t, $-CH_2Ar-$), 1.57−1.20 (9H, m, $C_4H_6 + CH_3$), 0.81 (3H, m, CH_3).

*4-(4′-Hexylphenylazo)phenyloxyacetate Acid (**3**).* Ethyl [4-(4′-hexylphenylazo)phenyloxy]acetate (2 g, 5.43 mmol) was hydrolyzed by refluxing it with 769 g (10.6 mmol) of sodium hydroxide in a mixture of ethanol (30 mL) and water (15 mL). After evaporation of the alcohol, the alkaline aqueous solution was rendered neutral using dilute hydrochloric acid up to a pH of 4−5. The product precipitated as a yellow solid and was purified by double recrystallization from methanol. Yield: 1.44 g (78%). ^{1}H NMR (DMSO): 13.2 (1H, br, −COOH), 7.82 (2H, d, J = 8.9 Hz, Ar−H), 7.24 (2H, d, J = 8.3 Hz, Ar−H), 7.23 (2H, d, J = 8.3, Hz, Ar−H), 6.93 (2H, J = 9.0 Hz, Ar−H), 4.87 (2H, s, $-OCH_2-$), 2.60 (2H, t, $-CH_2Ar-$), 1.57−1.35 (9H, m, C_4H_6), 0.92 (3H, m, CH_3).

*Pentafluorphenyl 4-(4′-Hexylphenylazo)phenyloxyacetate (**4**).* 4-(4′-Hexylphenylazo)phenyloxyacetate acid (1.38 g, 4.06 mmol) and pentafluorphenol (0.75 g, 4.05 mmol) were allowed to react in dry THF in the presence of dicyclohexylcarbodiimide (DCC) and a small amount of *p*-(dimethylamino)pyridine (DMAP) for 2 days. After separation of dicyclohexylurea by filtration, the solvent was removed by rotary evaporation. The resulting residue was purified by column chromatography on silica gel (eluent: ethyl acetate/*n*-hexane (v:v/1:6). The pure product is orange and crystalline. Yield: 1.44 g (68%). 7.83 (2H, d, J = 8.9 Hz, Ar−H), 7.25 (2H, d, J = 8.3 Hz, Ar−H), 7.24 (2H, d, J = 8.3, Hz, Ar−H), 6.94 (2H, J = 9.0 Hz, Ar−H), 4.88 (2H, s, $-OCH_2-$), 2.61 (2H, t, $-CH_2Ar-$), 1.57−1.36 (9H, m, C_4H_6), 0.92 (3H, m, CH_3).

*4-(4′-Hexylphenylazo)phenyloxyacetoyl-Functionalized Dendrimer (**5**).* PAMAM−$(NH_2)_{32}$ (795 mg, 0.11 mmol) with 32 primary amine groups (CAS: 204401-84-3) was dissolved in 10 mL of dried THF. To this solution was slowly added a solution of pentafluorphenyl [4-(4′-hexylphenylazo)phenyloxy]acetate (2.1 g, 4.1 mmol) in a dropwise fashion. After the addition was completed, the reaction mixture was refluxed for 2 days, yielding an orange solution. The solvent was removed by rotary evaporation and the obtained crude product was washed with diethyl ether twice to offer pure 4-(4′-hexylphenylazo)phenyloxyacetoyl-functionalized dendrimer as a yellow solid. Yield: 890 mg (yield, 78%). ^{1}H NMR ($CDCl_3$): 7.85 (128H, d, Ar−H), 6.94 (128H, d, Ar−H), 7.12 (t, 32H, NHCO), 4.80 (64H, s, $-OCH_2-$), 3.28 (64, m, CH_2NHCO), 2.60 (64H, t, $-CH_2Ar-$), 1.92−1.21(370H, m, $-(CH_2)_n-$), 0.84 (96H, m, CH_3). UV−vis (CH_2Cl_2): λ_{max} = 347 nm. The synthesis and grafting of the alternative reactive dye-B to the PAMAM dendrimer is under investigation (Figure 1).

General. The material used for a polymer matrix was polystyrene (PS) with an average Mw of 280 000 g/mol (Aldrich). Solvents for spin coating were HPLC-grade tetrahydrofuran (THF) and methylene chloride (CH_2Cl_2), purchased from Fisher Scientific.

Fabrication of Azobenzene-Modified PAMAM Films

For photoisomerization studies, doped polymer systems containing 5% and 50% (w/w) azo-dendrimer were prepared by dissolving the material in a 5% PS/THF (w/w) solution. Systems consisting of 100% azo-dendrimer were also prepared at 5 mg/mL in CH_2Cl_2. Previous screening using toluene, DMSO, and DMF as solutions and solvents for spin coating was not successful mainly because of differences in the solubility of the PAMAM−azo/PS materials in these solvents as well as heterogeneous films produced under these conditions. Poly(methyl methacrylate) (PMMA) was also investigated as a matrix polymer but with limited success arising from similar miscibility issues as mentioned above. Further studies will be done in this direction. For waveguiding experiments, systems containing 5% and 50% (w/w) azo-dendrimer were dissolved in a 50% PS/THF (w/w) solution. Sonication was employed to aid in the dissolution process. The solutions were filtered twice using 0.45-μm Millipore filters (Whatman). Thin films were prepared by the spin-coating technique onto glass substrates of area 3 × 3 cm, which were rotated at ≈2000 rpm for 1.5 min.

Instrumentation. UV−vis spectra were obtained using a Perkin-Elmer Lambda 20 spectrophotometer by employing an irradiation interrupt method. The incident light was aligned perpendicular to the substrate. The film was irradiated with a 150-W Hg lamp (Oriel) with a bandpass filter (350 nm). The optical output power was kept constant with the distance from the lamp being 10 cm. For the photoalignment procedure, the polarizer was placed between the sample substrate and the filter and set initially at $\theta = 0°$ phase for the parallel orientation of the irradiated light. Optical waveguide modes were performed using a Multiskop (Optrel, Germany) in the Kretschman configuration for doing ATR and prism coupling experiments. P-polarized light and s-polarized light from a He−Ne laser (632.8 nm) was used to illuminate the prism. The light signals were then converted (ac/dc) and digitized in a computer to produce a reflectivity angle of incidence scans. TEM images were obtained using a Hitachi transmission electron microscope (H-7000).

(17) Harke, M.; Teppner, R.; Schulz, O.; Motschmann, H.; Orendi, H. *Rev. Sci. Instrum.* **1997**, *68*, 3130.

(18) Knoll, W. *Annu. Rev. Phys. Chem.* **1998**, *49*, 569.

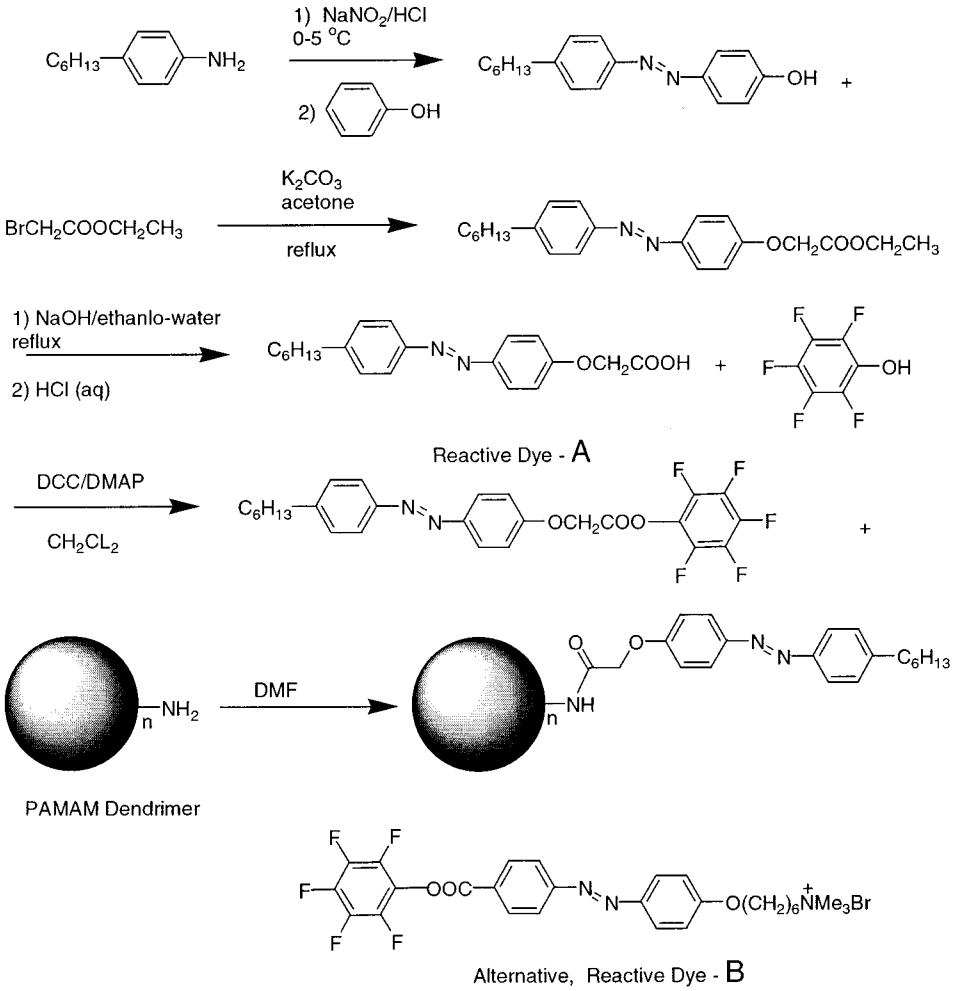

Figure 1. Synthesis of azobenzene-modified PAMAM dendrimers.

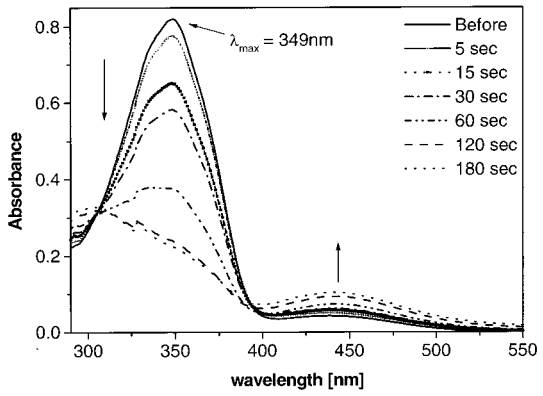

Figure 2. Time-dependent UV−vis absorption spectrum of PAMAM−azo in THF.

Results and Discussion

Photoisomerization in Solution. UV−vis sprectroscopy was primarily used to follow the process of photoisomerization of the azobenzene moieties. Photoisomerization of the azobenzene-functionalized PAMAM was observed in THF solution (10^{-7} M) at selected time intervals, as illustrated by the UV−vis spectra in Figure 2. Before irradiation with UV light, the observed spectrum was typical of azobenzene derivatives. The more stable trans isomer is characterized by a strong $\pi-\pi^*$ transition at 349 nm while the less stable cis isomer is characterized by a weak $n-\pi^*$ transition at ≈450 nm. Absorbance of the $\pi-\pi^*$ band at 349 nm progressively decreased with irradiation time, indicating a photochemical conversion from the trans to cis isomer configuration. Also observed was a progressive increase in the $n-\pi^*$ band associated with an increase of cis isomer within the system. After 3 min of irradiation, further significant changes in the spectra could not be detected, indicating the existence of a photostationary state containing 77% cis isomer. The fraction of cis isomers in the photostationary state was calculated from the absorbance at λ_{max} for the $\pi-\pi^*$ absorbance of the trans isomer at time t according to the equation[19]

$$[\text{cis}]_t/[\text{trans}]_0 = (1 - A/A_0)/(1 - \epsilon_{\text{cis}}/\epsilon_{\text{trans}}) \qquad (1)$$

where $[\text{cis}]_t$ is the concentration of cis isomer at time t, $[\text{trans}]_0$ is the initial concentration of the trans isomer, A_0 is the initial absorbance at λ_{max}, and (cis)/(trans) is the ratio of molar absorption coefficients of the cis and trans isomers at λ_{max}. For this study, the $\epsilon_{\text{cis}}/\epsilon_{\text{trans}}$ ratio was used in accordance with those values reported in the literature for similar types of systems.[20,21] Cis fractions in the photostationary state for other samples are summarized in Table 1.

Photoisomerization of Ultrathin Films. Irradiation has been performed on three different PAMAM−azo thin film systems: one containing only PAMAM−azo (100%,

(19) Imai, Y.; Naka, K.; Chujo, Y. *Macromolecules* **1999**, *32*, 1013.
(20) Morishima, Y.; Tsuji, M.; Kamachi, M.; Hatada, K. *Macromolecules* **1992**, *25*, 4406.
(21) Victor, J.; Torkelson, J. *Macromolecules* **1987**, *20*, 2241.

Table 1. Absorption Maximum Wavelength and Cis Fraction in the Photostationary State for All Samples

	λ_{max} (nm)	% cis isomer
PAMAM−azo (in THF)	349	77
100% PAMAM−azo (film)	342	47
50% PAMAM−azo/PS (film)	321	27
5% PAMAM−azo/PS (film)	323	24

no polymer matrix), one containing 50% PAMAM−azo, and one containing 5% PAMAM−azo, both spin-coated in a polymer (PS) matrix. The series of UV−vis spectra are shown in Figure 3a−b. Figure 3a shows the UV−vis spectra of the 100% PAMAM−azo thin film. In comparison to the PAMAM−azo spectrum obtained in THF solution, several differences can be noted after casting the system as a thin film. First, the $\pi-\pi^*$ band of the trans isomer is located at $\lambda_{max} = 341$ nm, shifted 8 nm blue from that in solution. This may be explained in terms of aggregation and will be discussed in detail below. Second, the efficiency of the photoisomerization process is reduced as seen by a smaller cis fraction (47%) in the photostationary state. This reduction of efficiency in the 100% PAMAM−azo system can be correlated to a decrease in the amount of free volume available for the photochemical conversion to occur. Logically, it can be assumed that the amount of free volume in the system is reduced when comparing the same molecule in solution and in a condensed thin film. This relationship of the photoisomerization of azobenzene moieties to available free volume has been reported on numerous occasions.[15,22]

Figure 3b shows the UV−vis spectra for the 50% PAMAM/PS (data for 5% PAMAM−azo/PS not shown). In a comparison of the absorption spectra of the PS-containing films with that of the PAMAM−azo in solution, several differences can be noted. In particular, the absorption maxims λ_{max} for the PAMAM−azo/PS films undergo a considerable hypsochromic (blue) shift in relation to the λ_{max} of PAMAM−azo in solution. A blue shift of 28 nm is observed for the 50% PAMAM−azo system and 26 nm for the 5% PAMAM−azo system. A similar shift was observed in the 100% PAMAM−azo system, only to a lesser extent with the spectrum showing an 8 nm blue shift. These spectral changes may be explained by considering the different aggregation states of the molecules. It is well-known that interchromophore interactions play an important role in the optical absorption of azobenzene chromophores.[23] According to the molecular exciton model, this shift to higher energy (blue) indicates that adjacent azobenzene chromophores are aggregated in such a way that their transition dipoles are parallel to one another. This type of interaction is known as H-aggregation. Otherwise, a bathochromic (red) shift is observed in the spectra when the adjacent azobenzene chromophores are J-aggregated or with an in-line alignment of transition dipoles. H-aggregation is commonly observed in well-ordered systems such as films prepared by the Langmuir−Blodgett technique while J-aggregation is most commonly associated with films of higher disorder such as spin-coated systems. In either case, H-type or J-type, the aggregation of azobenzene chromophores has been shown to restrict photoisomerization because of a limited amount of free volume within the aggregates.[24] All three of the thin films in this study, the 100% PAMAM−azo, 50% PAMAM−azo/PS, and 5% PAMAM−azo, exhibit this aggregation-related property. As mentioned previously, the cis fraction

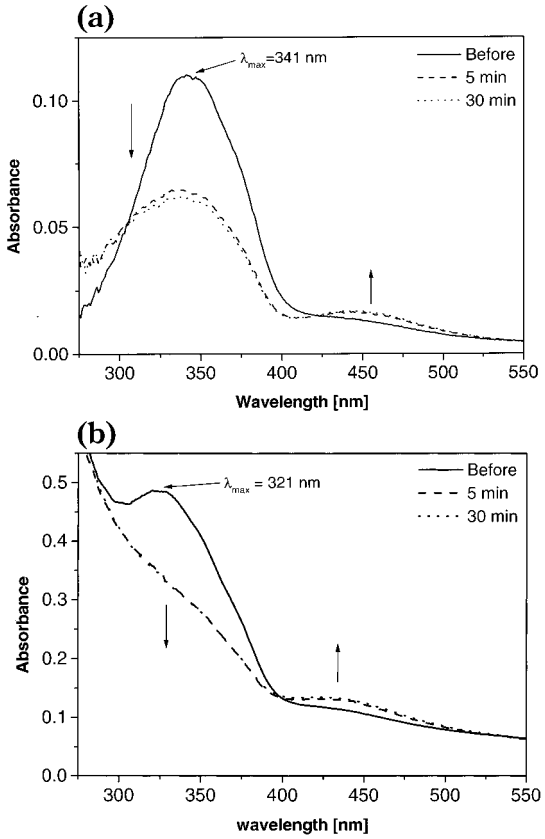

Figure 3. Time-dependent UV−vis absorption spectra for PAMAM−azo thin film systems: (a) 100% PAMAM−azo; (b) 50% PAMAM−azo/polystyrene.

for the 100% PAMAM−azo system was calculated to be 47% in the photostationary state. Likewise, a reduction in the photoisomerization process is observed as we increase the amount of PS in the system. Referring back to Table 1, the cis fraction for the 50% PAMAM−azo system was reduced to 27% and 24% cis isomer for the 5% PAMAM−azo system. Because the 5% PAMAM−azo system has less dendrimer embedded in the glassy PS thin film, the amount of free volume in the film is due primarily to the PS. This amount of free volume should be comparatively lower than the 50% PAMAM−azo system, which has a larger amount of the dendritic structure embedded in the thin film. This result shows a clear relationship between the efficiency of the photoisomerization process and the availability of free volume in the system as well as the aggregation state of the azobenzene molecules.

Photoinduced Alignment. Photoinduced alignment achieved by the irradiation of azobenzene chromophores in polymer films or tethered to polymer structures with linear polarized light results in the selective reorientation of the transition dipole of the chromophore into the direction perpendicular to the polarization vector of the incident light.[25] This results in a uniaxial orientation of the azo molecules, leading to photoinduced birefringence of azobenzene-doped polymer films. The polarized UV−vis spectra were obtained by recording the transmitted light both in parallel ($A_{||}$) and perpendicular ($A_{\perp}$) directions with respect to the direction of polarization. The isotropy of the films was checked before each experiment. Figure 4a,b (data for 5% PAMAM−azo not shown) shows the series of polarized UV−vis spectra for the thin film systems

(22) Kleideiter, G.; Sekkat, Z.; Kreiter, M.; Lechner, D.; Knoll, W. *J. Mol. Struct.* **2000**, *521*, 167.
(23) McRae, E. *J. Phys. Chem.* **1958**, *26*, 721.
(24) Wu, A.; Talham, D. *Langmuir* **2000**, *16*, 7449.
(25) Han, M.; Ichimura, K. *Macromolecules* **2001**, *34*, 90.

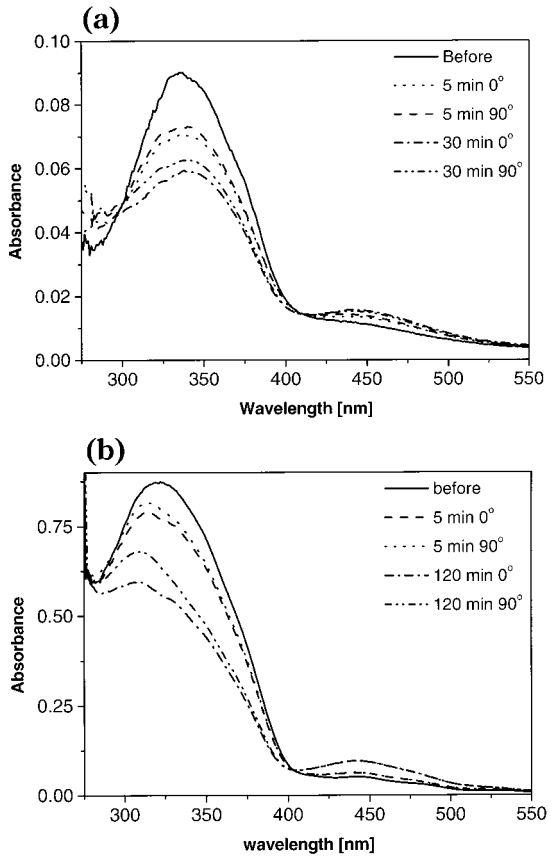

Figure 4. Polarized UV−vis absorption spectra for PAMAM−azo thin film systems: (a) 100% PAMAM−azo; (b) 50% PAMAM−azo/polystyrene.

Table 2. Calculated Dichroic Ratio

	2 min	photostationary state
100% PAMAM−azo (film)	1.0184	1.3028 (5 min)
50% PAMAM−azo/PS (film)	1.0367	1.1373 (120 min)
5% PAMAM−azo/PS (film)	1.0099	1.1683 (180 min)

under investigation. From these experiments, it was possible to observe a birefringence in each system and a dichroic ratio was calculated. By definition, the dichroic ratio is the ratio of the peak intensity for the s-polarized incident light to that of p-polarized light.[26] Table 2 shows a summary of the calculated dichroic ratios. A low level of dichroism was observed for each system at $t = 2$ min of polarized irradiation. As irradiation time increased, a larger difference in birefringence could be noticed between the pure 100% PAMAM−azo system and the blended systems containing PS. For example, the dichroic ratio at the photostationary state of the 100% PAMAM−azo system was calculated to be 1.3028, a value much higher than that found in the photostationary state for the 50% PAMAM−azo/PS system of 1.1373. Using a similar argument previously presented for the photoisomerization behavior, this difference in photoinduced alignment may be explained in terms of the reduction of available free volume in the system as we increase the amount of PS. Again, this directly relates to the aggregation state of the azobenzene chromophores. It should be pointed out that those chromophores with a transition dipole perpendicular to the polarization direction should not absorb light and thus should not undergo photoisomerization because the corresponding dipole momentum is equal to zero.[27] An interesting behavior was noticed with regard to the absorbance intensity ($A_\perp$) of the transmitted light in the direction perpendicular to the polarization vector. While we observed a decrease in parallel absorbance ($A_\parallel$) as expected (indication of photoismomerization of those azobenzenes with a dipole parallel to the polarization vector), we also observed a decrease in perpendicular absorbance ($A_\perp$). Cimrova et al. observed a similar behavior for nonmesogenic azobenzene-containing copolymers in which they attributed the behavior to either the formation of a second stable conformation of the nonmesogenic chromophore or photodegradation.[27] In our system, an explanation that considers the hyperbranched dendritic structure may be more appropriate. In light of the fact that all of the azobenzene chromophores are interconnected by the PAMAM dendrimer, this behavior may be indicative of a photoinduced cooperative motion between the photoactive and nonphotoactive azobenzene chromophores. This mechanism of cooperative motion and its effects on absorption spectra has been reported by Meng et al., in which they investigated the steric and polar factors affecting cooperative motion in amorphous polymers with azobenzene and nonphotochromic substituents.[28,29]

ATR Waveguide Spectroscopy. In polymer films of sufficient thickness, a type of nonradiative mode known as guided optical waves may be observed by the propagation of light through the film parallel to the substrate plane. For these waveguide modes to exist, the propagating light must fulfill the following condition,[30]

$$\beta_1 + \beta_2 + m\pi = k_z d \qquad (2)$$

where k_z is the wave vector of the mode in the z direction, d is the film thickness, m the mode order, and $2\beta_I$ the phase shifts occurring during reflection of the propagating light at the film boundaries. When the intensity of reflected light is recorded as a function of the angle of incidence θ, the excitation of optical waveguide modes are observed as narrow dips in the reflection curve. For thin layers, only surface plasmons (SP) can propagate along the metal−polymer interface. For thicker layers, it is possible to excite two sets of waveguide modes: transverse electric (TE), which are sensitive to the in-plane refractive index n_x perpendicular to the polarized light for photoisomerization and transverse magnetic (TM), which are sensitive to both in-plane refractive index n_y parallel to the light for photoisomerization and out-of-plane refractive index n_z in the direction normal to the waveguide plane.[27] A prism in optical contact with the substrate is used to couple freely propagating surface plasmons or guided waves. The spectrum was obtained by recording the reflectivity for incidence angles 30°−70°. The reflectivity curves for the 50% PAMAM−azo/PS system shown in Figure 5 were fitted according to Fresnel's formulas, which allowed the thickness and refractive indices in the three principle directions to be calculated. Using the change in refractive indices before and after UV irradiation, it is then possible to calculate a birefringence value for the system ($n_x - n_y$). The refractive indices and birefringence values are summarized in Table 3. Before exposure to UV radiation, equal

(26) Sutandar, P.; Ahn, D.; Franses, E. *Thin Solid Films* **1995**, *263*, 134.

(27) Cimrova, V.; Neher, D.; Kostromine, S.; Bieringer, Th. *Macromolecules* **1999**, *32*, 8496.

(28) Meng, X.; Natansohn, A.; Barrett, C.; Rochon, P. *Macromolecules* **1996**, *29*, 946.

(29) Menzel, H.; Ruther, M.; Stumpe, J.; Fischer, T. *Supramol. Sci.* **1998**, *5*, 49.

(30) Knobloch, H.; Orendi, H.; Buchel, M.; Seki, T.; Ito, S.; Knoll, W. *J. Appl. Phys.* **1995**, *77*, 2.

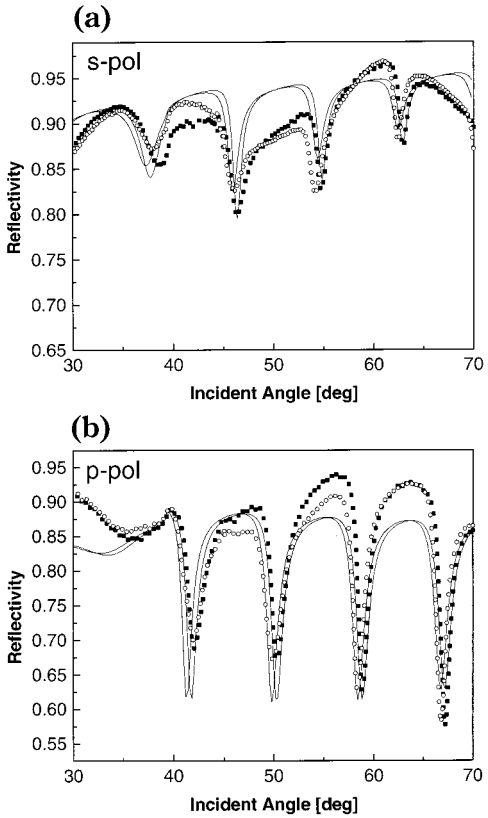

Figure 5. ATR reflectivity curves for (a) TE (s-pol) and (b) TM (p-pol) waveguide modes on 50% PAMAM−azo/PS before (square) and after (circle) irradiation with UV light. Solid curves are best experimental fits calculated using Fresnel formulas.

Table 3. Calculated Refractive Indices and Thickness for 50%PAMAM−azo/PS

polarization	irradiation time	n_x	n_y	n_z	$n_x - n_y$	thickness (nm)
TM (p-wave)	0 h	1.5047		1.500	0	2596
	4 h	1.5040		1.490		
TE (s-wave)	0 h		1.5047		0.0033	
	4 h		1.5007			

values of in-plane refractive indices (n_x, n_y) and a lower value of the out-of-plane refractive index (n_z) were recorded. This result is indicative of an initial out-of-plane anisotropy in the thin film, likely induced by the spin-coating process. After irradiation with UV light, decreases in all three refractive indices were detected. Polarized absorption experiments support this result, which showed a decrease in absorption for both in-plane polarization directions. The low birefringence value for the 50% PAMAM−azo/PS system is attributed to the H-aggregated state of the azobenzene chromophores. Results are shown only for the 50% PAMAM−azo/PS system because we were unable to observe a measurable change in the reflectivity for the 5% PAMAM−azo system. We believe this is due to a low chromophore content in the 5% system with the propagation of light due entirely to the polystyrene component. In the absence of PS, homogeneous films of 100% PAMAM−azo could not be obtained in sufficient thickness as to be characterized by the ATR waveguide technique.

Molecular and Matrix Interactions. Several factors influence the aggregation behavior observed for the azobenzene-functionalized dendrimers in this study. Among these factors is the molecular structure of the PAMAM dendrimer, intermolecular interactions between adjacent dendrimer molecules, and matrix−dendrimer interactions. Dendritic types of molecular architecture are becoming more prevalent as subjects of intense investigation in recent years. Some of these investigations are beginning to include microscopy techniques to visualize and understand the structural details of these molecules.[31−33] In particular, Tomalia et al. have visualized and characterized poly(amidoamine) dendrimers using the atomic force microscopy technique.[34] Using this technique, Tomalia's group was able to characterize individual PAMAM dendrimer molecules from generation five (G5) to generation ten (G10). For structures consisting of less than five generations of growth, it proved difficult to image individual molecules, even at very low concentrations. These images showed aggregation of the low-generation PAMAM dendrimers. The authors attribute this aggregation to an open and platelike structure of the lower generation dendrimer in which the branches of the molecule can interpenetrate one another and establish intermolecular interactions.[35] These intermolecular interactions should also play a role in our three-generation (G3) azobenzene-functionalized PAMAM dendrimer contributing to the interdigitation of the azobenzene chromophores. This interdigitation, as mentioned earlier, is evident in the UV−vis spectra of the PAMAM−azo thin films as indicated by the observed blue shift in the $\pi-\pi^*$ absorption peak.

Interactions between the polystyrene matrix and the PAMAM−azo dendrimer obviously play an important role in the thin film systems in this study. This excludes the 100% PAMAM−azo system in which dendrimer−dendrimer interactions would be expected to dominate the observed aggregation behavior. With the introduction of polystyrene into the system, we have competing interactions involving those between neighboring dendrimers as well as those between a less polar PS and a dendrimer of mixed polarity. Here, mixed polarity refers to the more polar PAMAM dendritic core and the less polar azobenzene functionalities. Given the observed ≈28-nm blue shift in the PAMAM−azo/PS systems and the mixed polarity of the PAMAM−azo molecule itself, it is feasible to assume phase separation may be induced within the system. This involves a micelle-like phase separation with a more polar PAMAM core and the less polar azobenzene chromophores interacting with the PS matrix. This type of model (illustrated in Figure 6b) would support the parallel interdigitation of the azobenzene chromophores, while those chromophores on the perimeter of the micelle-like structure would have more free volume to isomerize. To confirm the presence of phase separation and aggregation in the PAMAM−azo systems, we employed the transmission electron microscopy (TEM) technique. Using procedures reported in the literature, an aqueous solution of sodium phosphotungstate (NaPTA) was used, which resulted in a positively stained PAMAM dendrimer.[36] The dendrimers appear as dark objects on a light background of Formvar for the 100% system and polystyrene for the 5% system. Figure 6 shows the TEM micrographs of both the 100% PAMAM−azo thin film and the 5% PAMAM−

(31) Betley, T.; Banaszak, H.; Orr, B.; Swanson, D.; Tomalia, D.; Baker, J. *Langmuir* **2001**, *17*, 2768.
(32) Zhang, H.; Grim, P.; Foubert, P.; Vosch, T.; Vanoppen, P.; Wiesler, U. M.; Berresheim, A.; Mullen, K.; De Schryver, F. C. *Langmuir* **2000**, *16*, 9009.
(33) Hierlemann, A.; Campbell, J.; Baker, L.; Crooks, R.; Ricco, A. *J. Am. Chem. Soc.* **1998**, *120*, 5323.
(34) Li, J.; Piehler, L. T.; Qin, D.; Baker, J. R.; Tomalia, D. *Langmuir* **2000**, *16*, 5613.
(35) Naylor, A.; Goddard, W.; Kiefer, G.; Tomalia, D. *J. Am. Chem. Soc* **1989**, *111*, 2339.
(36) Jackson, C.; Chanzy, H.; Booy, F.; Drake, B.; Tomalia, D.; Bauer, B.; Amis, E. *Macromolecules* **1998**, *31*, 6259.

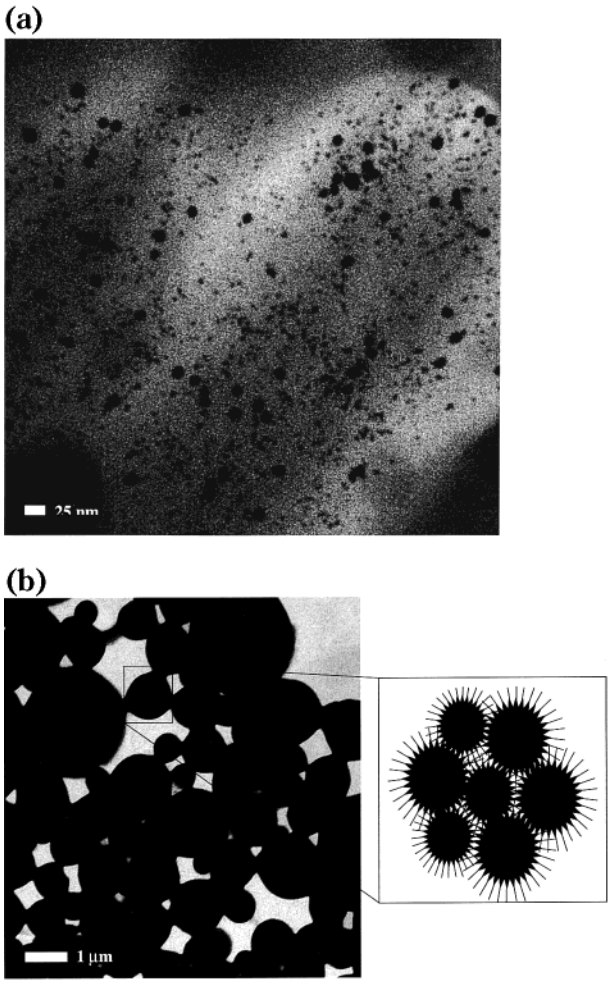

Figure 6. TEM images of PAMAM−azo dendrimers: (a) PAMAM−azo in the absence of polystyrene. The scale bar indicates 25 nm. (b) 5% PAMAM−azo/PS showing large aggregates of functionalized dendrimer. The scale bar indicates 1 μm. The outset in (b) shows a model of the micelle-like formation of PAMAM−azo within the aggregates.

azo/PS. The TEM image of the 100% PAMAM−azo system (Figure 6a) showed particles on the order of 4−5 nm in size. This is comparable to those values reported in the literature for dimensions of single dendrimer molecules.[35,36] Small amounts of larger particles can also be seen, which is indicative of aggregation and consistent with UV−vis data (8-nm blue shift) previously discussed for the 100% PAMAM−azo system. A vast difference in appearance of the TEM images is noticed as we look at the 5% PAMAM−azo/PS system. Phase separation of the PAMAM−azo dendrimer and PS matrix was observed as indicated by the positively stained dendrimer domains. Sizes of these domains varied but all were on the order of micrometers in dimension. Highly aggregated azobenzene domains have also been reported in mixed LB films consisting of semiamphiphilic stearoyl esters of Disperse Red-13 stearate (DR13st) and cadmium stearate.[37] Within these aggregated azobenzene domains, authors concluded that sufficient free volume did not exist for isomerization to occur. Although our system indicates the presence of these highly aggregated PAMAM−azo domains, a restricted amount of free volume is available for limited isomerization to occur.

Conclusion

In this work we describe the evanescent waveguide characterization and photoalignment of azobenzene-functionalized dendrimer ultrathin films. Azobenzene dyes were grafted to the perimeter of polyamidoamine (PAMAM) dendrimers. The photoisomerization and photoalignment properties were first investigated in relation to solution and film. The dendrimers were then blended with polystyrene, which served as a matrix for these investigations. Planar waveguides were prepared by spin coating the PAMAM−azo/PS systems onto Au−BK7 glass substrates. The waveguide structures were characterized by ATR methods sensitive to the s and p components of the waveguides, which allowed precise determination of the refractive indices of the films. The anisotropy of the dielectric constants were found to be highly dependent on the dendrimer/polystyrene ratio and aggregation properties of the functionalized dendrimers. The structure of the PAMAM−azo dendrimer and its molecular interactions within the system were identified as primary factors leading to the highly aggregated PAMAM−azo domains.

Acknowledgment. The authors gratefully acknowledge the American Chemical Society (PRF-35036-G7). D.P. also wishes to thank the National Science Foundation for financial support through the NSF GK-12 fellowship program. M.P. thanks Dr. Horst Orendi (Optrel GbR) for helpful discussions and technical assistance concerning waveguide techniques. We also acknowledge Leigh Millican (UAB High Resolution Imaging Facility) for assistance with the TEM imaging.

LA015622S

(37) Dos Santos, D. S., Jr.; Mendonça, C. R.; Balogh, D. T.; Dhanabalan, A.; Cavalli, A.; Misoguti, L.; Giacometti, J. A.; Zilio, S. C.; Oliveira, O. N., Jr. *Chem. Phys. Lett.* **2000**, *317*, 1.